HOW TO BREATHE IN A LIQUID-FILLED LUNG: SYMMETRY OF AIRWAY REOPENING.

Charles N. Baroud*, Matthias Heil**

*Laboratoire d'Hydrodynamique (LadHyX), CNRS-Ecole Polytechnique, F-91128 Palaiseau, France.

**Department of Mathematics, University of Manchester, Manchester M13 9PL, UK.

<u>Summary</u> Many respiratory diseases cause the occlusion of pulmonary airways with viscous fluid. The subsequent airway reopening is assumed to occur by the propagation of an air finger into the liquid-filled airways. We investigate the behavior of the air finger as it reaches a single bifurcation and determine under what conditions the finger branches symmetrically. If the fluid pressure in both channels ahead of the branching finger are equal, the finger will preferentially reopen a single path through the branching network. If the ends of the channels are capped with compliant chambers, representing the lung elasticity, the pressure required to drive the air finger can be dominated either by viscous losses or by elastic forces. Below a critical velocity, elastic forces dominate and symmetric branching is predicted to occur. We augment our theoretical model with an experimental study in which the problem is investigated using microfluidic channels.

MOTIVATION: THE LUNG AND THE MODEL

Many respiratory diseases, such as the Respiratory Distress Syndrome, may cause the occlusion of the pulmonary airways with viscous fluid. Occluded airways are believed to be reopened by a propagating air finger [1]. Previous models of pulmonary airway reopening (e.g. [2]) have only considered the propagation of air fingers in individual airway branches. Since the airways of the lung branch frequently, the question arises if the propagating air finger will reopen the whole lung tree or simply follow a single path, keeping most of the lung occluded.

We address this question at the level of a single bifurcation by modeling the flow of an air finger as it reaches a branching point, as shown in Fig. 1. An inviscid air finger propagates along a parent tube 1 of cross sectional area \mathcal{A} . The finger is driven by the injection of air at a constant flow rate, Q, and it displaces viscous fluid of viscosity, μ . The interfacial tension is σ . Downstream of the bifurcation, the lung's elasticity is represented by two compliant chambers whose volumetric elastic modulus is given by k.

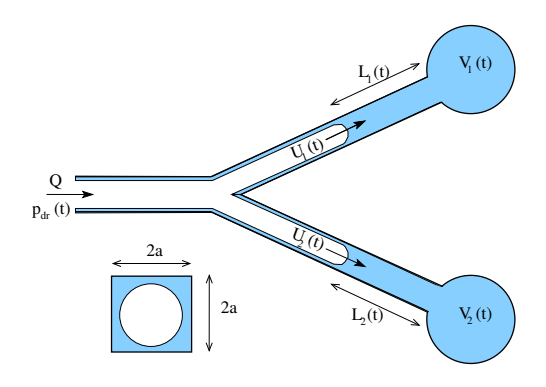


Figure 1. Model of a propagating finger through a single bifurcation.

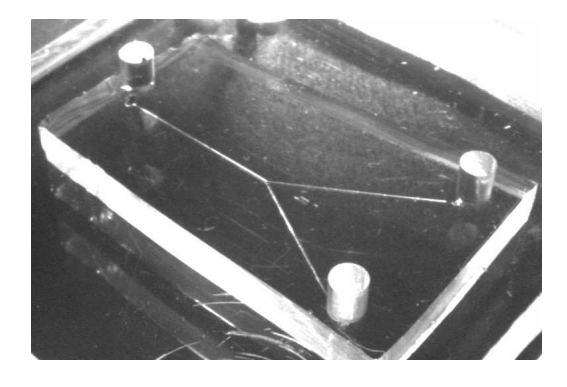


Figure 2. Experimental bifurcating channel, built using standard microfluidic technology.

MATHEMATICAL FORMULATION AND LINEAR STABILITY ANALYSIS

The flow rates in the two daughter tubes are given by $Q_i = U_i A_i$, where A_i is the cross-sectional area occupied by the air finger in daughter tube i. The sum of the flow rates in the daughter tubes must equal the incoming flux Q. The velocity of the finger tips is given by $U_i = -dL_i/dt$ where L_i is the length of the occluded section in daughter tube i. In the absence of inertial and gravitational effects, A_i is given by $A_i = \mathcal{A} \alpha(\operatorname{Ca}_i)$, where $\alpha(\operatorname{Ca}_i)$ is a function of the capillary number $\operatorname{Ca}_i = \mu U_i/\sigma$ and was computed in reference [3].

In each of the daughter branches, the pressure drop across the occluded section has three components:

- The viscous pressure drop through the liquid-filled section, $\Delta p_{\rm visc} = \mathcal{R}L_i(t)Q_i(t)$, where $\mathcal{R} \propto \mu/a^4$ depends on the geometry and the viscosity of the fluid.
- The capillary pressure drop across the curved tip of the air finger, $\Delta p_{\sf cap} = {\tt C}({\tt Ca}_i)$. Numerical results for $\Delta p_{\sf cap}$ are available from reference [3].
- The pressure $p_{\mathtt{elast}}$ in the elastic end-chambers. We assume that $p_{\mathtt{elast}}$ depends only on the injected volume such that $p_{\mathtt{elast}} = \mathcal{P}(V_{0i} + \int_0^t Q_i(\tau) d\tau)$ and we assume that $k = d\mathcal{P}(V)/dV = const.$

 $^{^1}$ To facilitate comparisons with the experiment, we consider the parent and daughter tubes to be rigid with square cross-section and constant cross-sectional area $\mathcal{A}=4a^2$; the analysis is easily extended to other geometries.

Since the air fingers in both daughter branches are subject to the same driving pressure $p_{dr}(t)$, we have

$$p_{dr}(t) = C(U_i) + \mathcal{R}L_i(t)Q_i(t) + \mathcal{P}(V_{0i} + \int_0^t Q_i(\tau)d\tau) \quad \text{for} \quad i = 1, 2.$$
 (1)

We differentiate Eq. 1 with respect to t, and use $U_i = -dL_i/dt$ and $Q_1 + Q_2 = Q$, to obtain a set of five ordinary differential equations with five unknowns: p_{dr} , U_1 , U_2 , L_1 and L_2 . These equations admit a symmetric solution of the form $U_i = \mathcal{U}$; the stability of this solution to small perturbations determines if the finger branches symmetrically or propagates along a single path.

A stability criterion for the symmetric solution is obtained using standard linear perturbation theory. Asymmetric perturbations are predicted to grow for positive values of the function

$$F(Ca) = \alpha(Ca) \left(2 - \frac{K}{Ca}\right) + Ca \frac{d\alpha(Ca)}{dCa} \left(1 - \frac{K}{Ca}\right), \tag{2}$$

where $\mathrm{Ca} = \mu \mathcal{U}/\sigma$ is the capillary number based on the propagation velocity of the symmetrically branching fingers; the dimensionless parameter $K = k\mu/\mathcal{R}\sigma$ indicates the importance of the elastic forces relative to viscous losses.

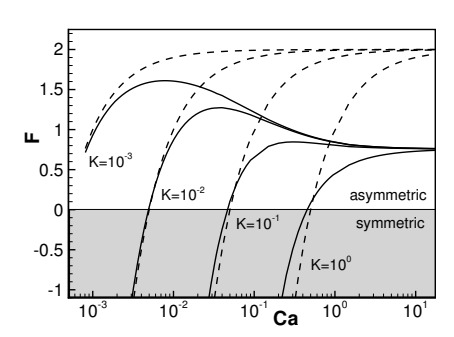


Figure 3. Variation of the function F with capillary number Ca: F < 0 corresponds to stable symmetric branchings, while F > 0 corresponds to asymmetric solutions. The dashed lines ignore capillary effects.

Figure 3 shows plots of F(Ca) for a range of values of the parameter K. For every value of K, there exists a critical value of Ca above which F > 0, and therefore symmetric solutions are unstable. Two special cases are noteworthy:

- 1. If we set $\alpha(\text{Ca}) = 1$ and C(Ca) = 0 and thus ignore the capillary effects, the predictions for F(Ca) are given by the dashed lines in Fig. 3. In this case it is possible to derive an explicit prediction for the critical velocity, $U_c = k/2\mathcal{R}$, such that for $\mathcal{U} > U_c$ the propagation is asymmetric, while $\mathcal{U} < U_c$ yields symmetric propagation. Figure 3 shows that U_c is an excellent approximation for the critical velocity predicted by the full analysis.
- 2. If we further ignore the compliance terms by setting k=0, we find that F>0 and the branching is *always* asymmetric.

EXPERIMENTAL METHODS AND PRELIMINARY RESULTS

The above mathematical model describes an actual experimental system, built using standard microfluidic soft lithography methods and shown in Fig. 2. The channel has a square cross-section with side $2a=100~\mu \mathrm{m}$ and total length 4 cm. It is initially filled with 100 cSt Silicone Oil, into which a water-fluorescein mixture is injected using a computer-controlled micropump. The injection rate varies in the range $0.3-3~\mu \mathrm{L/min}$. The elasticity of the end chambers is achieved through the use of thin membranes with variable thickness and diameter, so as to yield different values of K. The fluorescent finger is followed as it advances through the bifurcation for different flow rates, in order to determine the symmetry of the branching.

A preliminary experimental image is shown in Fig. 4. Here, the end-chambers have no compliance but are open to the atmosphere, corresponding to special case 2 above. We obtain experimentally that the branching is always asymmetric

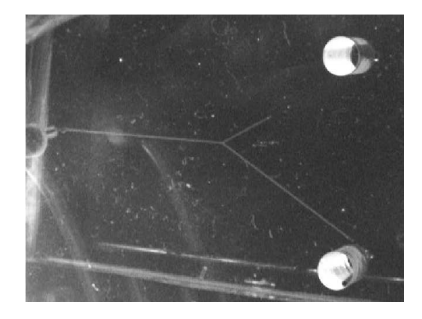


Figure 4. Asymmetric branching in openended microchannel

case 2 above. We obtain experimentally that the branching is always asymmetric, as expected from the analysis. Further experiments are currently being conducted with the elastic chambers to verify the theoretical predictions above.

CONCLUSIONS

Our model predicts two distinct régimes for air fingers penetrating liquid-filled networks. The behavior that is chosen depends on the relative dominance of the viscous vs. the elastic forces. In the case when viscous effects are dominant, an air finger will follow a linear path in the network, leaving the other branches occluded. Future work aims to investigate the application of similar models to real lungs in order to understand the reopening of fluid-filled airways in living organisms.

References

- [1] D.P. Gaver, R.W. Samsel, and J. Solway. Effects of surface tension and viscosity on airway reopening. J. Appl. Physiol., 369:74-85, 1990.
- [2] A.L. Hazel and M. Heil. Three-dimensional airway reopening: The steady propagation of a semi-infinite bubble into a buckled elastic tube. *J. Fluid Mech.*, 478:47–70, 2003.
- [3] A.L. Hazel and M. Heil. The steady propagation of a semi-infinite bubble into a tube of elliptical or rectangular cross-section. *J. Fluid Mech.*, 470:91–114, 2002.